

Forward Physics and BRAHMS results

Ramiro Debbe[†] for the BRAHMS Collaboration

[†] Brookhaven National Laboratory, Upton NY, 11973

Abstract. We report here the BRAHMS measurements of particle production in d+Au and p+p collisions at RHIC. The results presented here are compared to previous p+A measurements at lower energies in fixed target mode. Some preliminary results on abundances of identified particles at high rapidity are also presented.

1. Introduction

The first collisions of gold ions at nucleon-nucleon center of mass energies $\sqrt{s_{NN}} = 130\text{GeV}$ at RHIC showed a dramatic drop in the production of pions at intermediate p_T compared to an incoherent sum of pions produced in p+p collisions at the same energy (approximately a factor of 5 for the most central collisions) [1]. The measured suppression could be the result of energy degradation of jets traversing a newly formed dense medium or could also be related to modifications to the wave function of the ions brought in by the high energy of the collisions together with the high atomic number A of the nuclei [2]. Collisions between deuterium and gold ions at $\sqrt{s_{NN}} = 200\text{GeV}$ were produced during the third RHIC run to resolve the apparent conflict between the above mentioned explanations of the suppression. Particle production from d+Au collisions around mid-rapidity do not show the suppression seen in Au+Au collisions [3, 4]. What is seen instead is an enhancement that has been associated with the so called “Cronin effect” [5], where partons undergo multiple incoherent scatterings that increase their transverse momenta as they traverse through the target. These results constitute evidence that a new dense and highly opaque medium has been formed in Au+Au collisions at RHIC [6] and the suppression of intermediate to high p_T leading particles is directly related to their interaction with that medium be it collisional or by induced gluon radiation.

But the unexpected low overall multiplicities seen in Au+Au collisions points to a strong degree of coherence compatible with the onset of saturation in the wave function of the ions. A saturation that appears below a transverse momentum scale whose value increases with the energy of the collisions and the atomic number ($A=197$) of the colliding nuclei.

Asymmetric reactions like the d+Au run in collider mode (as is the case at RHIC) are fertile ground for QCD studies firstly because projectile and target fragmentation regions are well separated. Furthermore, detection of particles in the fragmentation regions skews even more the kinematics at the partonic level. (See appendix A). These asymmetric systems are thus ideal to study the small- x components of the Au target wave function.

2. Lower energy p+A measurements

Before proceeding with the description of BRAHMS studies of d+Au collisions, a brief review of previous measurements is necessary to emphasize the novelty of the results that we are going to

present. Early studies of p+A collisions were conducted with the primary aim of extracting the proton energy loss in nuclear matter. All those measurements were done in fixed target mode. I base this review in two well know reviews [7, 8]. Compared with the RHIC measurements, all these experiments suffer from the fact that in fixed target mode the projectile fragmentation region (close to the proton rapidity) is boosted to very small angles and a detailed transverse momentum dependent studies were just not possible.

Many of these measurements have concentrated in particle production as function of polar angle or pseudo-rapidity $\eta = -\log(\tan\frac{\theta}{2})$.

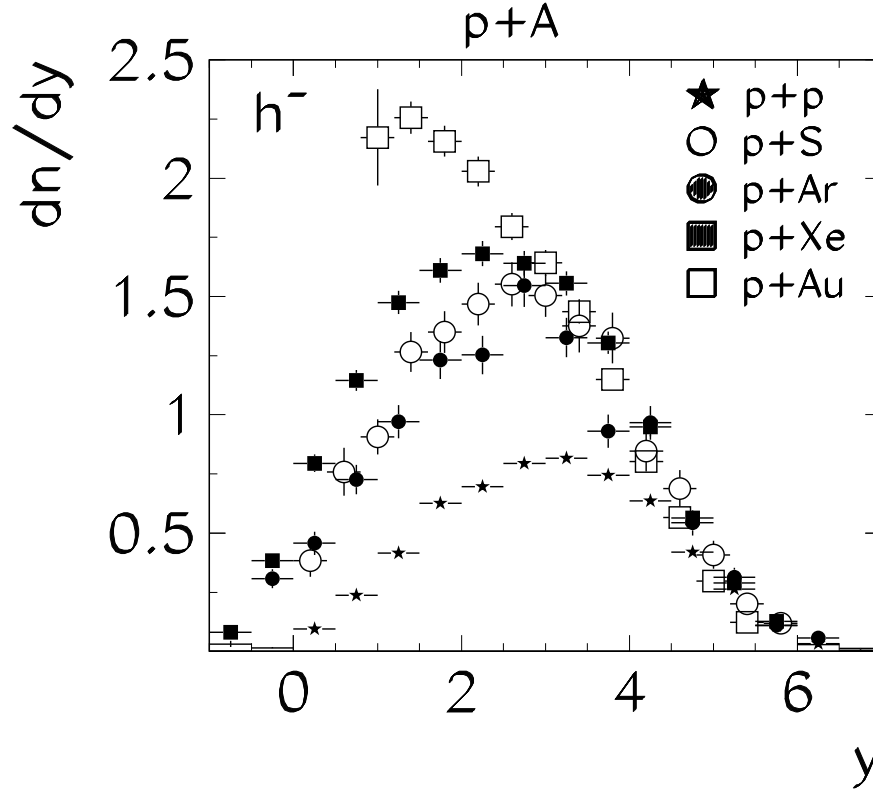


Figure 1. Rapidity distribution for negative particles (mostly negative pions) produced in p+p and p+A collisions at $\sqrt{s_{NN}} = 19.4 \text{ GeV}$ at the SPS [10]

Figure 1 shows two main features: the first being the fact that most of the yield (in this particular case, negative particles or mostly pions) from p+A collisions appears close to the target fragmentation regions (y or $\eta \sim 0$ in the lab. reference frame) and the second is the fact that within ~ 1 unit of rapidity close to beam rapidity, the projectile proton has no more “memory” of the target. Similar behavior has been shown to be independent of the beam energy (see one such compilation done in the projectile reference frame [8]). If the yields from p+A collisions are compared to those from p+p at same energy one obtains a characteristic wedge like distribution that has been explained in the context of multiple parton interactions; the projectile appears as if it had only one interaction but can interact with several target nucleons. The ratio starts at $\eta = 0$ with a value equal to the numbers of partonic interactions and ends at the rapidity of the projectile with a value equal to one. [9].

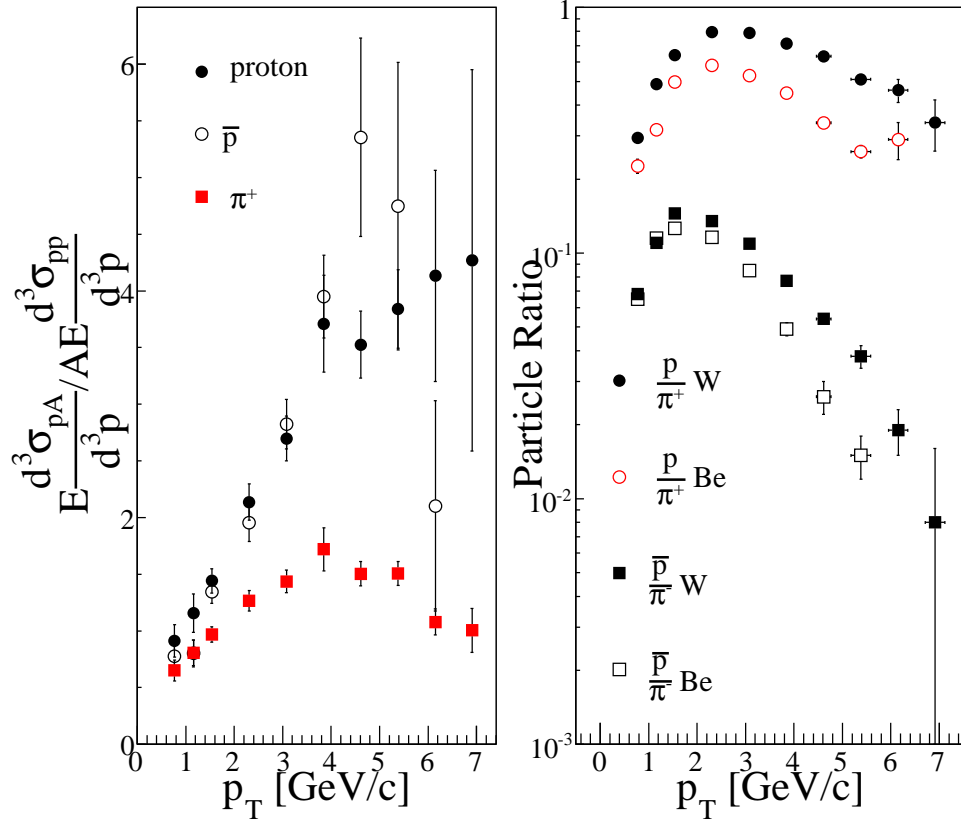


Figure 2. Left panel: Nuclear modification factor for pions, protons and anti-protons at mid-rapidity in p+W at $\sqrt{s_{NN}} = 27.4 GeV$. For protons and anti-protons some of the data was collected at rapidities smaller but close to mid-rapidity. Right panel: Ratios of baryon to mesons around mid-rapidity. [5]

The measurements of hadrons at large transverse momentum done at Fermilab [5] have shown what is now called the Cronin effect; an enhancement that is widely considered as incoherent multiple elastic interactions as the projectile moves through the target, each one of these interactions modifies the transverse momentum distributions by shifting counts from low p_T values up to intermediate values ($\sim 4-5 GeV/c$). The nuclear modification factor defined as a ratio of differential cross sections normalized by the atomic number A of the targets is used to compare to an incoherent sum of p+p collisions at the same energy, is shown in the left panel of Fig. 2. The ratio for pions has a clear enhancement that starts above 2 and extends to 7 GeV/c. Anti-protons show a strikingly different behavior when compared to the above described pions. The difference between baryon and meson present at this energy $\sqrt{s_{NN}} = 27.4 GeV$ has also been seen at RHIC. The right panel of the figure shows a comparison of abundances of baryons (protons and anti-protons) and mesons (pions). The ratio of anti-proton to negative pions is small and consistent with hadronization in the vacuum, the ratio of protons to positive pions, is greater and approaches one for the heaviest target. Because of the energy of the collisions it may be that this ratio is affected by beam protons. Some degree of stopping is expected to transfer protons to mid-rapidity where this ratio was constructed.

In Figure 3 we show results from collisions at even lower energy. This time, the nuclear

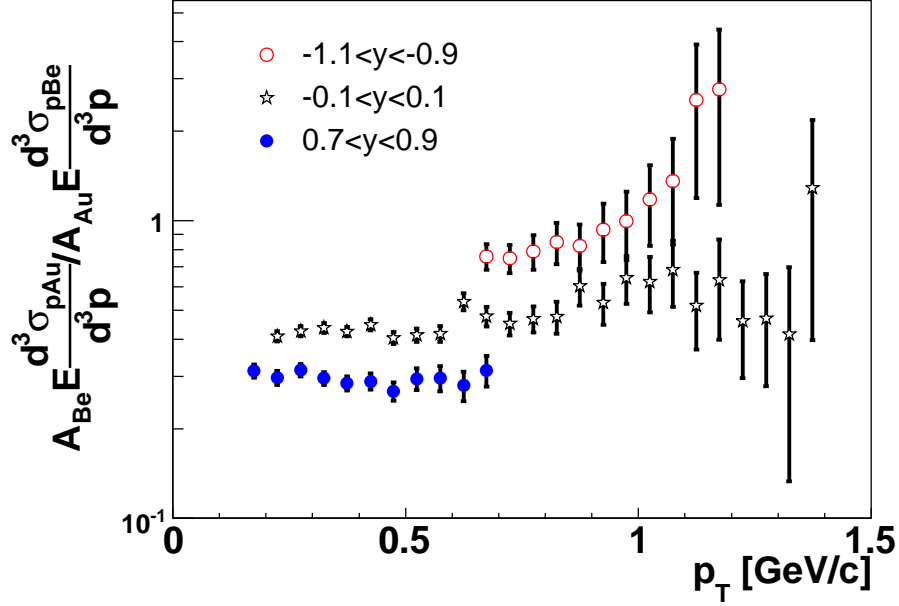


Figure 3. Nuclear modification factor constructed from invariant cross sections for positive pions produced in p+Au and p+Be collisions at $\sqrt{s_{NN}} = 5\text{GeV}$ at the AGS ($y_{CM} = 1.7$) [11]

modification factor is defined as a ratio of invariant differential cross sections for positive pion production scaled by the atomic number of the targets. The comparison is done between a heavy target (Au) and a light one (Be). The data was collected in fixed target mode at the AGS with the E802 spectrometer. The large acceptance coverage in rapidity provides some access to both target and projectile fragmentations regions. The rapidity of the 14.6 GeV/c proton beam is equal to 3.4 and the figured is labeled with the rapidities in the nucleon-nucleon center of mass ($y_{CM} = 1.7$).

The most striking feature of this figure is the fact that the curves are arranged in the same descending order as the above mentioned “triangular distribution”. Only the ratio calculated close to target rapidities ($-1.1 < y < -0.9$) crosses the value of 1 at $p_T \sim 1\text{GeV}/c$. The ratios corresponding to mid-rapidity $y = 0$ and $y \sim 1$ have values smaller than one. According to the scattering models used to explain the Cronin effect the low momentum (ratio below 1) is depleted because each rescattering shifts the event to higher p_T bins. The depletion is stronger as the rapidity increases because the reach into lower values of x in the target wave function is greater; more scattering centers are thus available. Naive scattering models imply that at higher rapidities, the Cronin peak appears at higher values of p_T , however, data extending to high p_T values is not available. It should also be said that available phase space puts limits the application of such arguments.

3. Intermediate p_T studies and the nuclear modification factors

BRAHMS is one of the four RHIC experiments with the unique capability to measure identified hadrons with transverse momenta that can reach moderately high values ($\sim 5\text{GeV}/c$) and can access rapidities close to the beam rapidity ($y=5.4$ for the 100 GeV/c per nucleon beam). The

data that is described in this presentation is thus a first detailed study of particle production in the beam fragmentation region in d+Au collisions at the highest energy in the center of mass. As such, the data may be a window to new phenomena and in particular, it has been listed as a first indication that the small- x components of the target wave function have entered a non-linear mode. The data collected from d+Au collisions is compared to p+p using the so called nuclear modification factor defined as: $R_{dAu} = \frac{1}{N_{coll}} \frac{\frac{dN^{dAu}}{dp_T d\eta}}{\frac{dN^{pp}}{dp_T d\eta}}$. If the target is already a saturated system of gluons, the ratio is expected to show a decrease in value as the rapidity of the detected particles increases. If the target is a dilute system of gluons the ratio should grow with rapidity because at higher rapidities, the detected particle has interacted with a higher number of small- x gluons each contributing a finite amount of transverse momentum, such that the ratio never gets smaller than one.

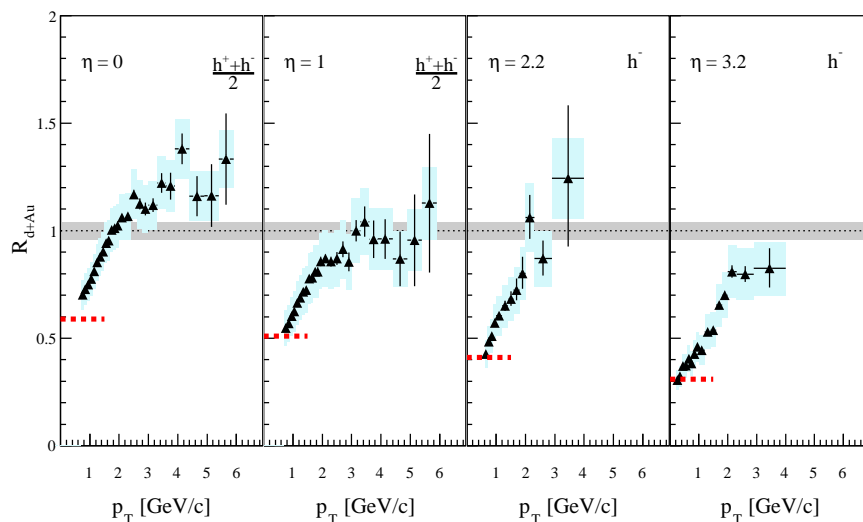


Figure 4. Nuclear modification factor for charged hadrons at pseudorapidities $\eta = 0, 1.0, 2.2, 3.2$. Statistical errors are shown with error bars. Systematic errors are shown with shaded boxes with widths set by the bin sizes. The shaded band around unity indicates the estimated error on the normalization to $\langle N_{coll} \rangle$. Dashed lines at $p_T < 1$ GeV/c show the normalized charged particle density ratio $\frac{1}{\langle N_{coll} \rangle} \frac{dN/d\eta(d+Au)}{dN/d\eta(pp)}$.

Figure 4 shows the nuclear modification factor with the number of binary collisions set to $N_{coll} = 7.2 \pm 0.6$ for minimum biased d+Au collisions. This particular study was done without identifying the particles. Each panel shows the ratio calculated at a different pseudo-rapidity η values. At mid-rapidity ($\eta = 0$), the nuclear modification factor exceeds 1 for transverse momenta greater than 2 GeV/c in similar way as the pions in figure 2.

One unit of rapidity towards the deuteron rapidity is enough to make the enhancement disappear, and then become consistently smaller than 1 for the next two values of pseudo-rapidity ($\eta = 2.2$ and 3.2) indicating a suppression in d+Au collisions compared to scaled p+p systems at the same energy.

The novelty of this result stands mainly on the fact that the measurement extends to moderate transverse momenta (~ 3.5 GeV/c) and the factor appears consistently suppressed for all value of p_T , specially at $\eta = 3.2$.

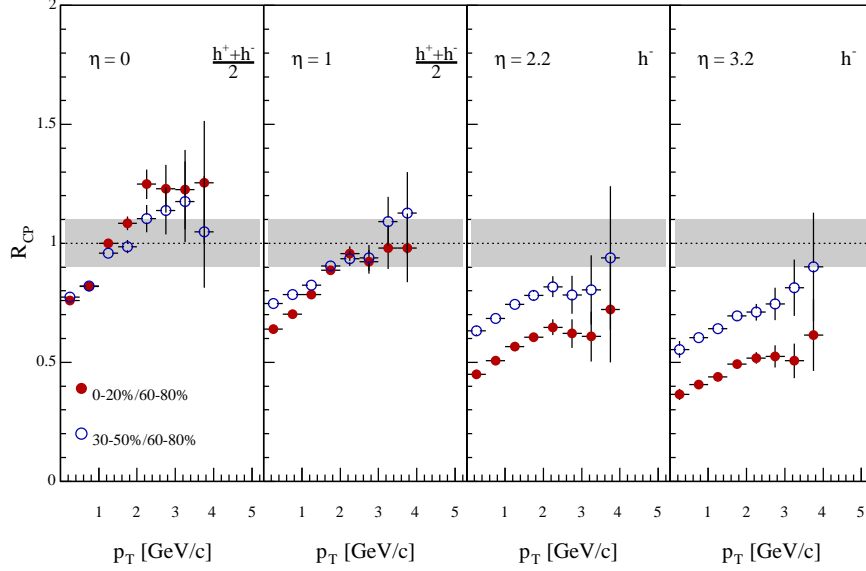


Figure 5. Central (full points) and semi-central (open points) R_{cp} ratios (see text for details) at pseudorapidities $\eta = 0, 1.0, 2.2, 3.2$. Systematic errors ($\sim 5\%$) are smaller than the symbols. The ratios at the highest pseudorapidities ($\eta = 2.2$ and 3.2) are calculated for negative hadrons. The uncertainty on the normalization of the ratios is displayed as a shaded band around unity. Its value has been set equal to the error in the calculation of N_{coll} in the most peripheral collisions (12%).

The four panels of Fig. 5 show the central $R_{CP}^{central}$ (filled symbols) and semi-central $R_{CP}^{semi-central}$ (open symbols) ratios for the four η settings. Central events have a higher number of target nucleons participating in the interaction with the deuteron projectile. This higher number of nucleons translates into an increase in the number of gluons present in the system and if the conditions are set for saturation, central collisions would have stronger suppression as function of rapidity. If the target is still a linear dilute system the $R_{CP}^{central}$ would be enhanced as function of rapidity because of the higher number of scattering centers that become available in the target. In the left panel of Fig. 5 corresponding to $\eta = 0$, the yield from 5 is systematically higher than those of the semi-central events, but at the highest pseudo-rapidity $\eta = 3.2$, the trend is reversed; the yields from central events are $\sim 60\%$ lower than the semi-central events at all values of p_T . More details on these results can be found in [12]. These results have been described within the context of the Color Glass Condensate [13] and its evolution with rapidity where gluon fusion becomes dominant is consistent with the suppression seen in central events at the highest pseudo-rapidity measured [14].

The difference between mesons and baryons seen at lower energies and shown for pions and anti-protons in Fig. 2 has also been found at RHIC energies at all rapidities, in particular, Fig. 6 presents the minimum bias nuclear modification R_{dAu} for anti-protons and negative pions at $\eta = 3.2$. These ratios were obtained making use of ratios of raw counts of identified particles compared to those of charged particles in each p_T bin:

$$R_{dAu}^{\bar{p}} = R_{dAu}^{h^-} \frac{(\frac{\bar{p}}{h^-})^{dAu}}{(\frac{\bar{p}}{h^-})^{pp}} = \frac{1}{N_{coll}} \frac{\frac{dn^{dAu}}{dp_T d\eta}^{h^-}}{\frac{dn^{pp}}{dp_T d\eta}^{h^-}} \frac{\frac{dn^{dAu}}{dp_T d\eta}^{\bar{p}}}{\frac{dn^{pp}}{dp_T d\eta}^{\bar{p}}} = \frac{1}{N_{coll}} \frac{\frac{dn^{dAu}}{dp_T d\eta}^{\bar{p}}}{\frac{dn^{pp}}{dp_T d\eta}^{\bar{p}}}$$

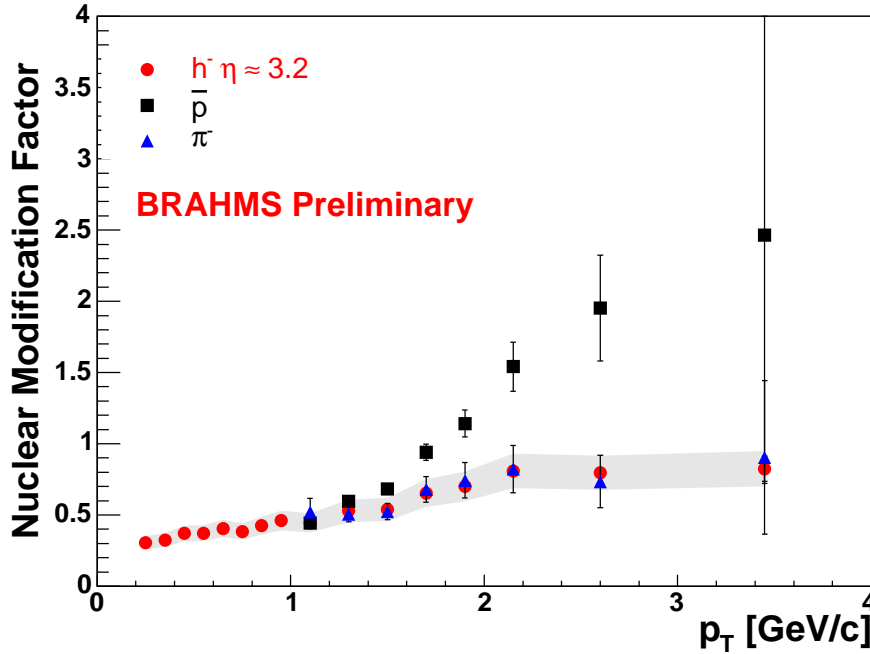


Figure 6. The nuclear modification factor R_{dAu} calculated for anti-protons (filled squares) and negative pions (filled triangles) at $\eta = 3.2$. The same ratio calculated for negative particles at the same pseudo-rapidity [12] is shown with filled circles, and the systematic error for that measurement is shown as grey band.

No attempt was made to estimate the contributions from anti-lambdas feed down to the anti-proton result. The remarkable difference between baryons and mesons has been related to parton recombination [15].

The ratios shown in Fig. 7 show a new aspect of particle production at forward rapidities. The left panel shows that at $\eta = 3.2$ the yield of protons is comparable to that of pions ($\sim 80\%$) while the yield of positive kaons hovers around 40%. These results indicate that even though pion production is well described at all rapidities in p+p collisions [17], the presence of so many baryons at that rapidity brings additional complications to NLO pQCD calculations, which cannot be reconciled with the data if standard fragmentation functions are used [18]. Panel a of Fig. 7 shows that, there are as many protons as positive pions ($\sim 80\%$ at $p_T \sim 2 \text{ GeV}/c$) in the positive particle distribution at $\eta = 3.2$. The abundance of baryons at this high energy and rapidity doesn't support the idea of baryon suppression in the fragmentation region [19, 20] where, because of their high energy, the quarks of the beam would fragment independently

mostly into mesons. But if that suppression was actually present close to beam rapidity, baryon number conservation would force the transfer of beam protons to lower rapidities, what remains a mystery is how did these protons acquire the high transverse momentum ($\sim 2\text{GeV}/c$ that is measured. The panel b of Fig. 7 a similar baryon excess in p+p collisions at the same high rapidity. This time the comparison is made to Pythia simulations.

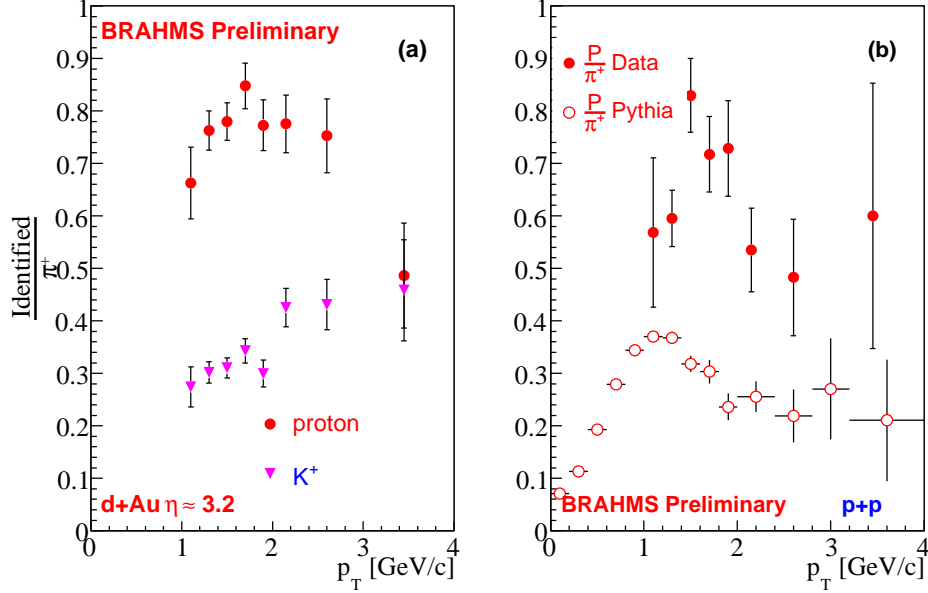


Figure 7. The fraction of proton over positive pions at $\eta = 3.2$: (a) Particle composition of positive charged hadrons produced in d+Au collisions at $\eta = 3.2$. The abundance of protons and kaons are compared to the one of pions as function of transverse momentum. (b) The same comparison but this time for particles produced at the same rapidity and energy in p+p collisions.

In summary, the study of particle production from d+Au and p+p collisions at $\sqrt{s_{NN}} = 200\text{GeV}$ and different rapidities with the BRAHMS setup takes advantage of the asymmetry of these reactions to reach the small-x components in the Au wave function. The suppression found at high rapidities may be the first indication of the onset of saturation in the gluon distribution function in the target.

4. Acknowledgments

This work was supported by the Office of Nuclear Physics of the U.S. Department of Energy, the Danish Natural Science Research Council, the Research Council of Norway, the Polish State Committee for Scientific Research (KBN) and the Romanian Ministry of Research.

References

- [1] K. Adcox *et al.*, PHENIX Collaboration, Phys. Rev. Lett. **88** 022301 (2002);
- [2] D. Kharzeev, E. Levin, and L. McLerran, Phys. Lett. B **561**, 93 (2003).
- [3] B.B. Back *et al.*, PHOBOS Collaboration, Phys. Rev. Lett. **91**, 72302 (2003); S.S. Adler *et al.*, STAR Collaboration, Phys. Rev. Lett. **91**, 72303 (2003); J. Adams *et al.*, PHENIX Collaboration, Phys. Rev. Lett. **91**, 72304 (2003).
- [4] I. Arsene *et al.*, BRAHMS Collaboration, Phys. Rev. Lett. **91**, 072305 (2003).

- [5] D. Antreasyan *et al.*, Phys. Rev. D **19**, 764 (1979).
- [6] PHENIX Collaboration nucl-ex/0410003; I. Arsene *et al.*, BRAHMS Collaboration, Nucl. Phys. A **757** 1-27, nucl-ex/0410020 (2004).
- [7] S. Fredriksson *et al.*, Phys. Rep. **144** 187-320 (1987).
- [8] W. Busza and R. Ledoux, Ann. Nucl. Part. Sci. **38** 119 (1988).
- [9] S. Brodsky, Gunion and Khun Phys. Rev. Lett. **39**, 1120 (1977).
- [10] T. Alber *et al.*, NA35 Collaboration, hep-ex/9711001.
- [11] T. Abbott *et al.*, E802 Collaboration, Phys. Rev. D **45**, 3906 (1992).
- [12] I. Arsene *et al.*, Phys. Rev. Lett. **93**, 242303 (2004).
- [13] L. McLerran and R. Venugopalan, Phys. Rev. D **49**, 2233 (1994), Phys. Rev. D **49**, 3352 (1994), Phys. Rev. D **50**, 2225 (1994), Phys. Rev. D **59**, 094002 (1999); Y. V. Kovchegov, Phys. Rev. D **54**, 5463 (1996), Phys. Rev. D **55**, 5445 (1997).
- [14] D. Kharzeev, Y. V. Kovchegov and K. Tuchin Phys. Rev. D **68**, 094013, (2003), hep-ph/0307037; D. Kharzeev, E. Levin and L. McLerran, Phys. Lett. B **561**, 93 (2003); R. Baier, A. Kovner and U. A. Wiedemann Phys. Rev. D **68**, 054009, (2003); J. Albacete, *et al.* hep-ph/0307179.; A. Dumitru and J. Jalilian-Marian, Phys. Lett. B **547**, 15 (2002); J. Jalilian-Marian, A. Kovner, A. Leonidov, H. Weigert, Phys. Rev. D **59**, 014014 (1999). J. Jalilian-Marian *et al.* Phys. Lett. B **577**, 54-60 (2003), nucl-th/0307022;
- [15] R. C. Hwa, C. B. Yang and R. J. Fries Phys. Rev. C **71**, 024902, (2005).
- [16] K. Adcox *et al.*, PHENIX Collaboration, Phys. Rev. Lett. **88** 022301 (2002); S. S. Adler *et al.*, STAR Collaboration, Phys. Rev. Lett. **89** 202301 (2002); B.B. Back, *et al.*, PHOBOS Collaboration, Phys. Lett. B **578**, 297 (2004).
- [17] J. Adams *et al.* Phys. Rev. Lett. **92**, 171801, (2004).
- [18] V. Guzey, M. Strikman, W. Vogelsang, Phys. Lett. D **603**, 173 (2004).
- [19] A. Dumitru, L. Gerland, and M. Strikman hep-ph/0211324, (2003).
- [20] A. Berera *et al.* Phys. Lett. B **403**, 1-7, (1997).

Appendix A. Kinematics of pA

The Parton model describes hadrons moving at very high momentum as combinations of systems of massless partons in numbers that grow as the energy of the probe increases. Each parton carries a fraction x of the hadron momentum P . (Because of the very high momentum of the hadron any transverse motion can be neglected.)

Let S be the total center-of-mass energy squared: $S = (\mathbf{P}_A + \mathbf{P}_B)^2$ where \mathbf{P}_A and \mathbf{P}_B are four vectors. (Naturally the beam momentum defines one preferred direction, and from now on we state that the four-momenta \mathbf{P}_A and \mathbf{P}_B have only one component along that direction. If the momenta of the colliding nucleons is high compared to their masses, one can neglect the masses and write:

$$S = (E_A + E_B)^2 - (\vec{P}_A + \vec{P}_B)^2 = m_A^2 + m_B^2 + 2E_A E_B - 2\vec{P}_A \cdot \vec{P}_B \equiv 2\mathbf{P}_A \cdot \mathbf{P}_B$$

The masses of the nucleons can be neglected ($E = P$ for both nuclei and $P_A = -P_B$) and one writes in the center of mass of the collision:

$$S = 4P_A P_B$$

The fraction x of the hadron's longitudinal momentum carried by each parton is defined as the ratio of the parton and hadron longitudinal momenta: $x \equiv \frac{p_{parton}^{\parallel}}{P_{hadron}}$.

If we define \hat{s} as a quantity related to S but only including the longitudinal component of the momenta:

$$\hat{s} = (e_a + e_b)^2 - (p_a^{\parallel} + p_b^{\parallel})^2 = M^2 + (p_a^T + p_b^T)^2 = M_T^2$$

and because p_a and p_b are anti-parallel the cross term of the sum of momenta squared is positive:

$$\hat{s} = 2x_1 x_2 P_A P_B + 2e_a e_b$$

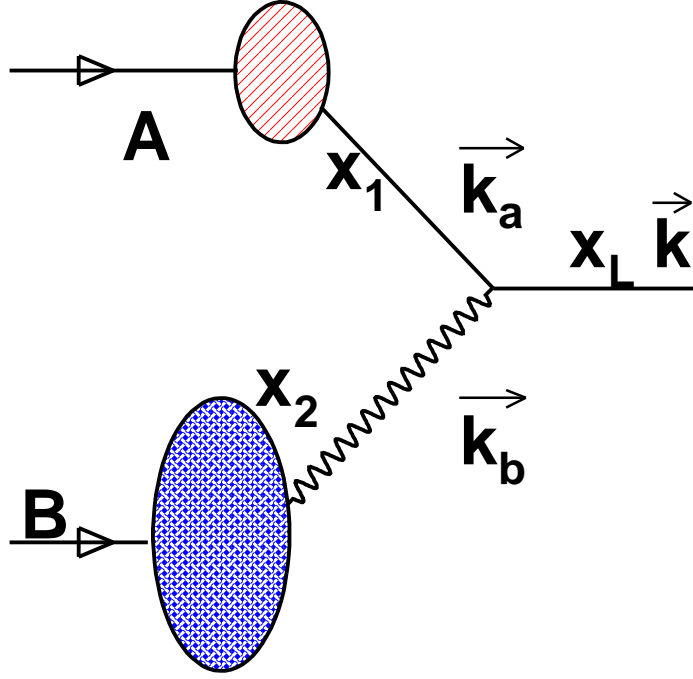


Figure A1. Diagram representing a $2 \rightarrow 1$ process in a collision between two nucleons A and B. The detected particle has longitudinal momentum fraction x_L and rapidity y .

where x_1 is the longitudinal momentum fraction of the projectile parton, and x_2 is the longitudinal momentum fraction of the target parton. If we neglect the masses of the partons and their transverse momentum components: $e_a = p_a^\parallel$ and $e_b = p_b^\parallel$ we obtain the relation between \hat{s} and S the total energy in the center of mass of the nucleons:

$$\hat{s} = x_1 x_2 S = M_T^2$$

On the other hand, if the detected particle has rapidity y and longitudinal momentum p_L its longitudinal momentum fraction is defined in the center-of-mass frame as: $x_L = \frac{2p_L}{\sqrt{S}}$ longitudinal momentum conservation for the 2 to 1 process is written as:

$$x_1 - x_2 = x_L = \frac{2M_T}{\sqrt{\hat{s}}} \sinh y$$

and together with the relation between energy in the nucleon-nucleon center of mass S and the one in the parton-parton system, we have a system of two equations with two unknowns x_1 and x_2 .

$$x_1 = \frac{M_T}{\sqrt{S}} e^y$$

$$x_2 = \frac{M_T}{\sqrt{S}} e^{-y}$$

It is now clear how the work at high rapidities opens a window into the low values of x_2 in the target wave function.